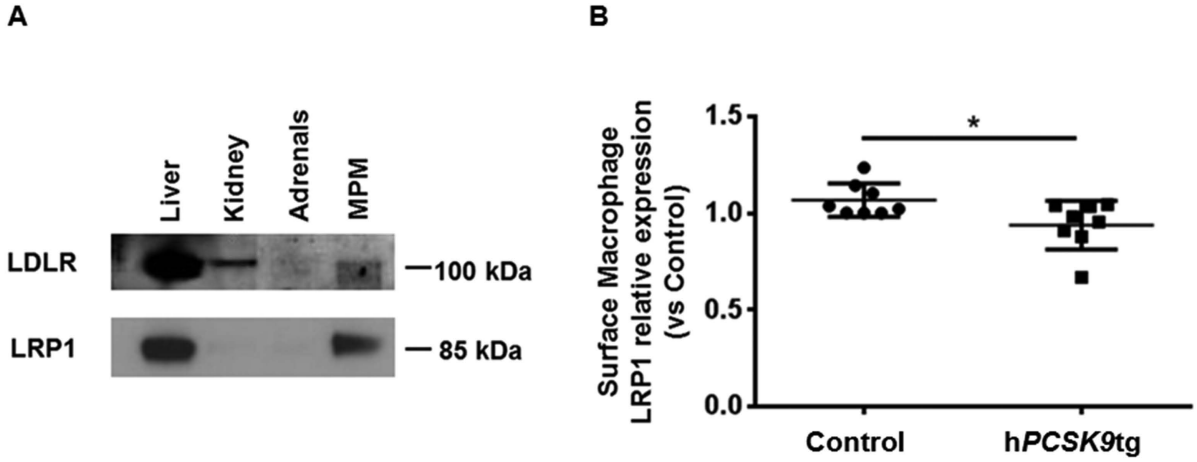

Supplementary Figure 1. (A) Immunoprecipitation of hPCSK9 in liver, kidney, adrenals and MPM collected from h*PCSK9*tg mice and relative western blot analysis of LDLR and LRP1 (B) Flow cytometry analysis of surface LRP1 levels in MPM from apoE$^{-/-}$ or h*PCSK9*tg/apoE$^{-/-}$ mice.

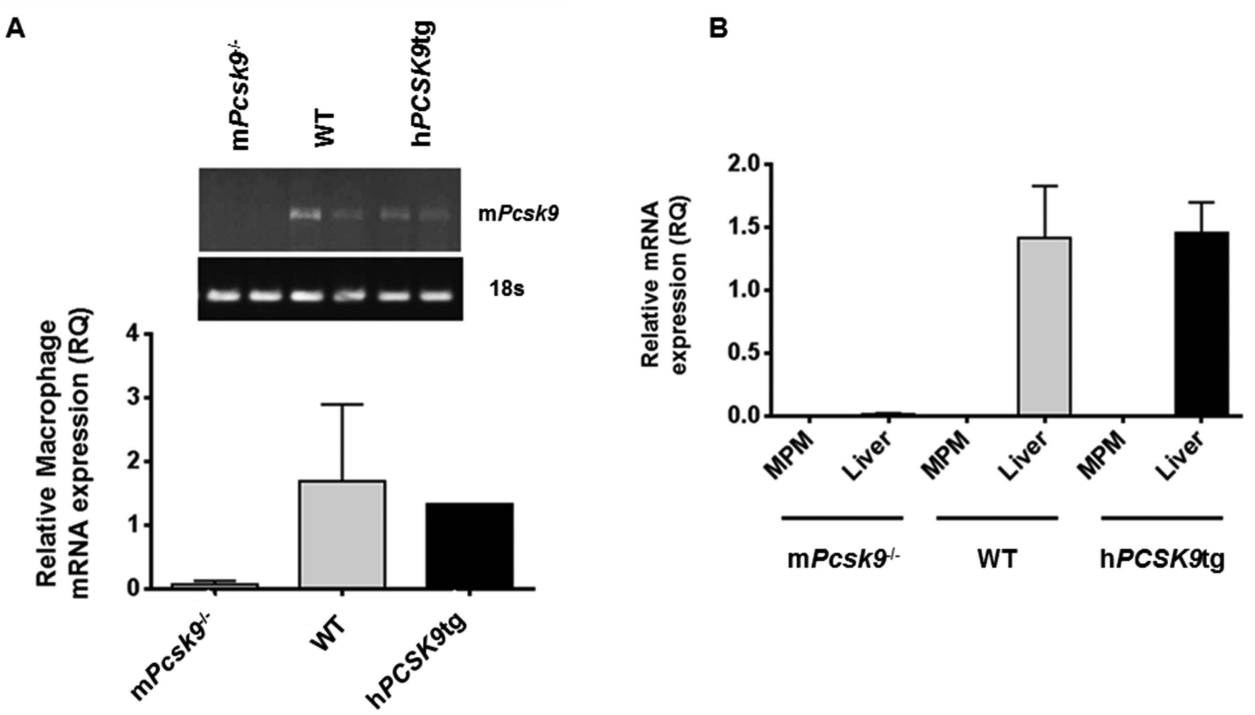

Supplementary Figure 2. (A) Relative mRNA levels of m*Pcsk9* in MPM from m*Pcsk9*$^{-/-}$, WT and h*PCSK9*tg mice, as measured by PCR. (B) Relative mRNA levels of m*Pcsk9* in MPM and livers from m*Pcsk9*$^{-/-}$, WT and h*PCSK9*tg mice, as measured by QRT-PCR.

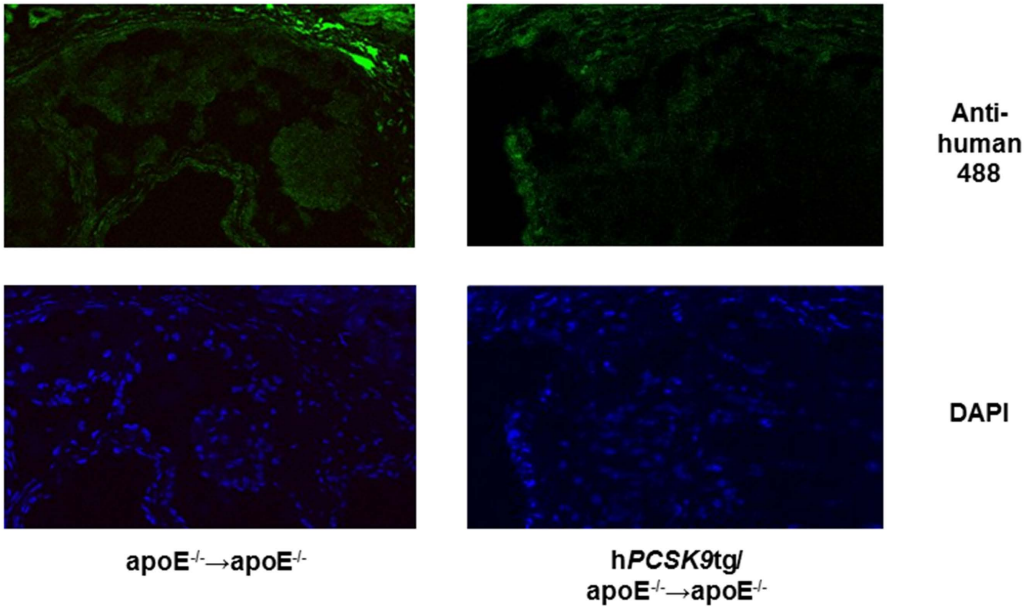

Supplementary Figure 3. Representative images showing negative control staining of lesions of proximal aortas in apoE$^{-/-}$→apoE$^{-/-}$ or h*PCSK9*tg/apoE$^{-/-}$→apoE$^{-/-}$ mice. In green: anti-human secondary antibody staining; in blue: DAPI.

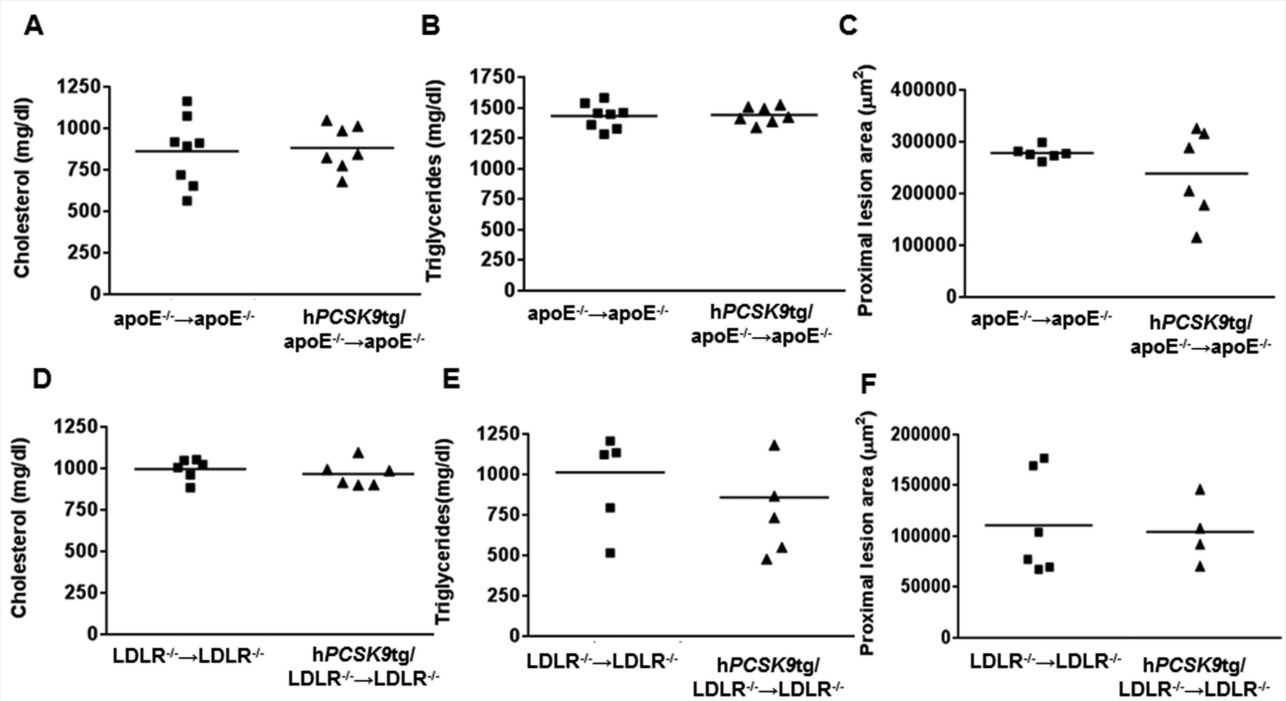

Supplementary figure 4. (A) Total serum cholesterol levels measured in apoE$^{-/-}$→apoE$^{-/-}$ or h*PCSK9*tg/apoE$^{-/-}$→apoE$^{-/-}$ (B) Serum triglyceride levels measured in apoE$^{-/-}$→apoE$^{-/-}$ or h*PCSK9*tg/apoE$^{-/-}$→apoE$^{-/-}$ (C) Quantitation of proximal lesion area in Oil red O stained proximal aortas of apoE$^{-/-}$→apoE$^{-/-}$ or h*PCSK9*tg/apoE$^{-/-}$→apoE$^{-/-}$ mice (D)Total serum cholesterol levels measured in LDLR$^{-/-}$→LDLR$^{-/-}$ or h*PCSK9*tg/LDLR$^{-/-}$→LDLR$^{-/-}$ mice (E) Serum triglyceride levels measured in LDLR$^{-/-}$→LDLR$^{-/-}$ or h*PCSK9*tg/LDLR$^{-/-}$→LDLR$^{-/-}$ mice (F) Quantitation of proximal lesion area in Oil red O stained proximal aortas of LDLR$^{-/-}$→LDLR$^{-/-}$ or h*PCSK9*tg/LDLR$^{-/-}$→LDLR$^{-/-}$ mice.

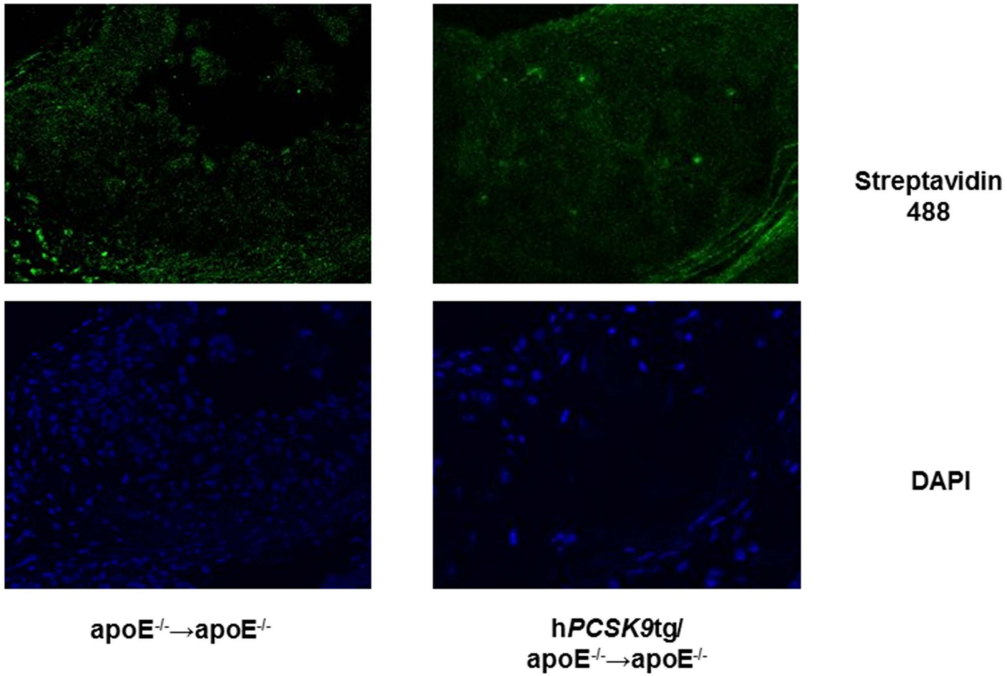

Supplementary Figure 5. Representative images showing negative control staining of lesions of proximal aortas in apoE$^{-/-}$→apoE$^{-/-}$or h*PCSK9*tg/apoE$^{-/-}$→apoE$^{-/-}$ mice. In green: streptavidin 488 antibody staining; in blue: DAPI.

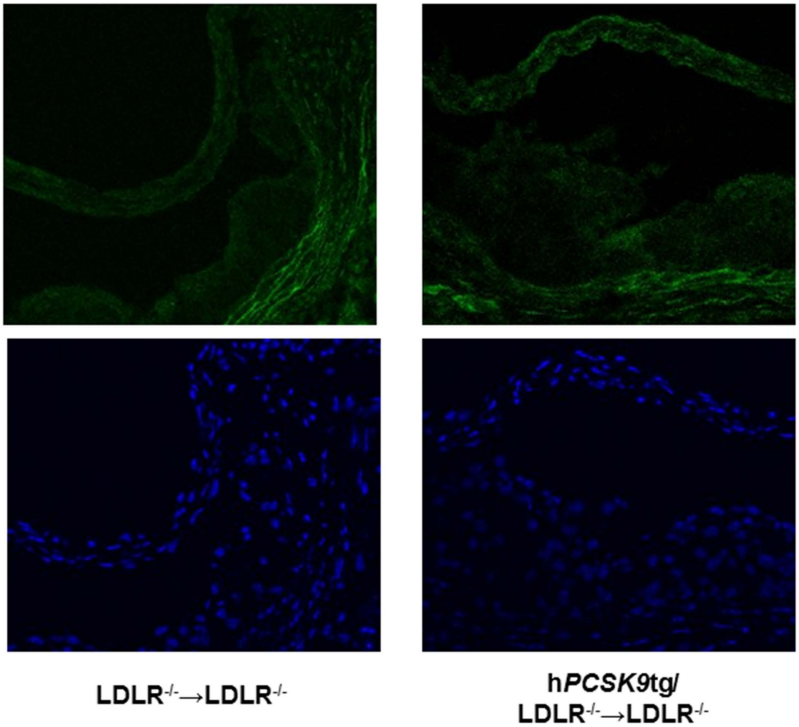

Supplementary Figure 6. Representative images showing negative control staining of lesions of proximal aortas in LDLR$^{-/-}$→LDLR$^{-/-}$or h*PCSK9*tg/LDLR$^{-/-}$→LDLR$^{-/-}$ mice. In green: anti-human secondary antibody staining; in blue: DAPI.

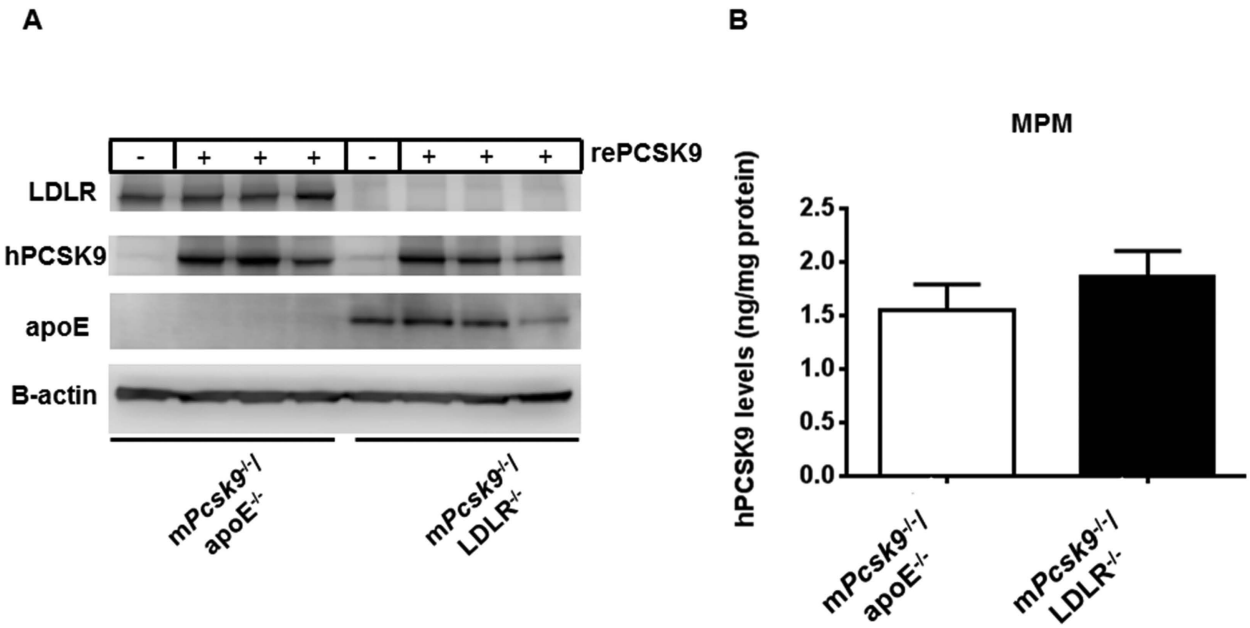

Supplementary figure 7. (A) Western blot analysis of hPCSK9, LDLR and apoE in MPM from m*Pcsk9*$^{-/-}$/LDLR$^{-/-}$ or m*Pcsk9*$^{-/-}$/apoE$^{-/-}$ mice incubated overnight with recombinant hPCSK9 (rePCSK9) 1000ng/ml (B) Quantification of intracellular levels of hPCSK9 in MPM from m*Pcsk9*$^{-/-}$/LDLR$^{-/-}$ or m*Pcsk9*$^{-/-}$/apoE$^{-/-}$ mice incubated overnight with rePCSK9 1000ng/ml.

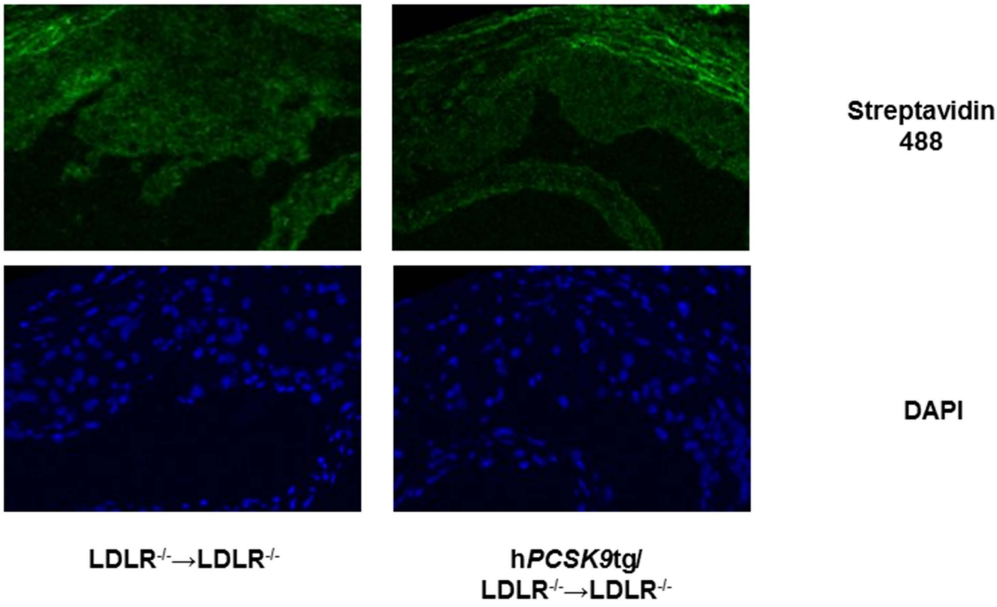

Supplementary Figure 8. Representative images showing negative control staining of lesions of proximal aortas in LDLR$^{-/-}$→LDLR$^{-/-}$or h*PCSK9*tg/LDLR$^{-/-}$→LDLR$^{-/-}$ mice. In green: streptavidin 488 antibody staining; in blue: DAPI.

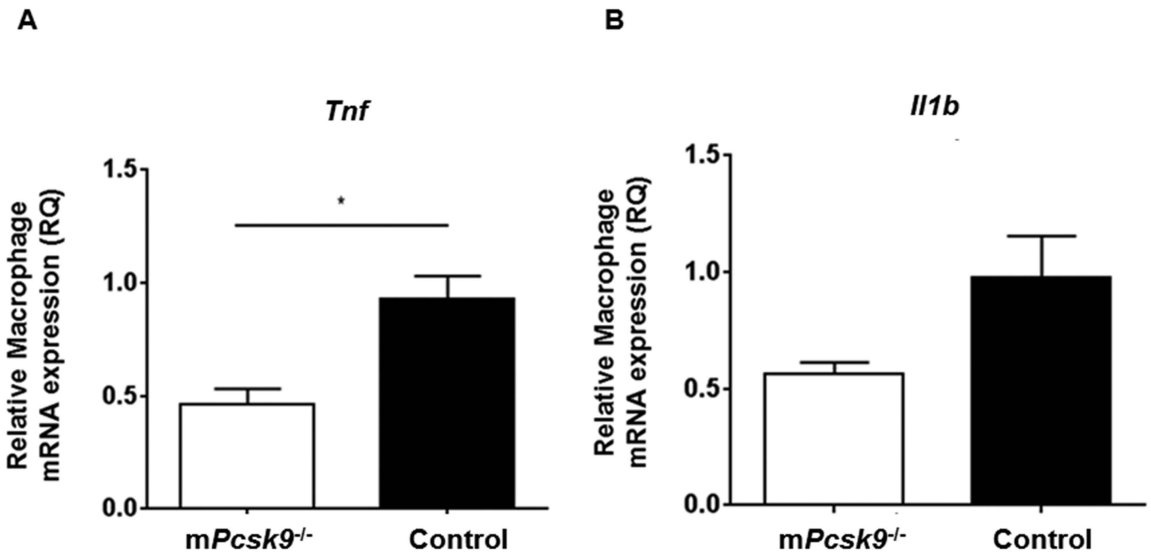

Supplementary figure 9. mRNA expression of *Tnf* (A) and *Il1b* (B) in LPS-stimulated MPM from m*Pcsk9*$^{-/-}$ and Control mice